FRACTURE MECHANICS PROPERTIES OF MATERIALS OF REACTOR PRESSURE VESSEL OF WWER 440

D. Lauerová, M. Brumovský

Nuclear Research Institute Řež plc, 25068 Řež, Czech Republic

ABSTRACT

In the paper, evaluation of 9 large scale experiments performed on uncladded cracked beams made of RPV WWER 440 materials (base and weld metal, in initial and aged condition) is described. The experiments were performed with the aim to determine values of fracture mechanics parameters, such as J_c/K_{Jc} and Q [1,2], and to compare the obtained J_c/K_{Jc}-values with the data obtained from standard (small scale) tests. Using „Master curve" approach (adjusting data to 1T thickness and using reference temperature T_o) enabled plotting the data from both large scale and standard tests for all materials into one figure and the effect of crack depth could be examined. The elevated values of J were found for beams containing shallow cracks. For two of specimens containing shallow through cracks, also the Q-stress parameter was calculated. A qualitatively correct relation between elevation of fracture toughness J_c/K_{Jc} and loss of constraint expressed by negative values of Q was found for these two specimens. The evaluation of the experiments is not completed to date and creation of the database of J_c/K_{Jc} and Q-values will continue in the future.

INTRODUCTION

Recently, series of 16 large scale experiments on beams made from materials of reactor pressure vessel of WWER 440 were performed in Nuclear Research Institute Řež plc, Czech Republic. Both cladded and uncladded beams were tested. The experiments were performed with the goal to obtain large scale experimental data related to assessment of integrity of RPV, in particular, critical values of fracture mechanics parameters, such as J_c/K_{Jc} and, in some cases, Q [1, 2]. J_c/K_{Jc} values were compared with results of standard (small scale) tests. The effect of crack depth, specimen size and cladding were intended to be examined.

Four types of materials were tested: base metal of RPV WWER 440, i.e. ferritic steel of 15Kh2MFA grade (Cr-Mo-V type), in initial and aged condition, and weld metal, in initial and aged condition. Under aged condition the simulated material degradation close to the end of pressure vessel life is understood.

In the paper, the results of only 9 large scale experiments performed on uncladded beams are described. The effect of crack depth on fracture toughness is studied; K_{Jc} remains as a main fracture mechanics parameter, and two-parameter fracture mechanics approach (J-Q) has been also applied. In our case, the calculations of Q-stress parameter were performed only for the uncladded specimens containing through cracks, and since the calculations are not fully completed to date, only results for two specimens are presented in this paper.

SPECIMEN CONFIGURATION AND TESTING FACILITY

In the experiments, 16 beams of basic dimensions 70(thickness) x 102(width) x 670(length) were tested. The beams contained relatively shallow (with a/W ratio varying in range 0.11 to 0.29) cracks of through or semi-elliptical shape. Half of the specimens were cladded with two layer austenitic cladding. From each group (cladded or uncladded) again one half contained through crack and one half contained semi-elliptical crack. The overview of geometrical as well as material conditions of the specimens is presented in the following Table 1. (The true crack dimensions were slightly different from those presented in the Table 1.)
The cracks, both through and semi-elliptical, were introduced into the specimens by fatigue pre-cracking. In the case of underclad cracks the specimen was first fatigue pre-cracked and then cladded. Two layers of austenitic cladding were applied, the total thickness of cladding being 8 mm (the total thickness of cladded specimen was thus 78 mm). The specimens contained either realistic type defects (size 8 x 24 mm), or postulated type defect (size 15 x 45 or through-crack of 15 mm deep).
For testing of the specimens, a special testing facility was used, originally constructed for testing of cruciform specimens. This facility permits besides biaxial loading of cruciform specimens also uniaxial loading of beams. In the case, the active load is developed through 2 hydraulic cylinders, the central support is of a form of circular pillar (ended on the top by a square seat) and passively reacts the loading applied. The result is that the large scale beam specimen is tested under 4 point bending.

TABLE 1
MATERIAL AND GEOMETRICAL CHARACTERIZATION OF THE TESTING SPECIMENS

Material			Specimen			
material notation	material type	material condition	semi-elliptical cracks		through cracks	
			crack size (mm)			
A	base metal	initial	PHAV201 surface crack 15 x 45	PHAV202 underclad 15 x 45	PHAV103 surface crack 15	PHAV104 underclad 15
B	base metal	aged	PHBV101 surface crack 8 x 24	PHBV102 underclad 8 x 24	PHBV103 surface crack 15	PHBV104 underclad 15
C	weld metal	initial	PH1C101 surface crack 15 x 45	PH1CV102 underclad 15 x 45	PH1CV103 surface crack 15	PH1CV104 underclad 15
D	weld metal	aged	PH3DV101 surface crack 8 x 24	PH3DV102 underclad 8 x 24	PH3DV103 surface crack 15	PH3DV104 underclad 15

MATERIAL PROPERTIES

The overview of material properties for individual specimens is attached in Table 2.

TABLE 2
MATERIAL PROPERTIES OF SPECIMENS

Specimen (or group of specimens)	Test temperature, °C	Young modulus, E, GPa	Poisson ratio, ν	Yield Strength, $R_p0.2$, MPa	Ultimate Tensile Strength, R_m, MPa	Uniform Elongation, A_m, %
PHA	- 120	210	0.3	683	797	9.5
PHBV101 PHBV103 PHBV104	+ 24			841	918	5.2
PHBV102	- 40			875	962	5.4
PHC	+ 24			519	597	9.2
PH3DV101 PH3DV104	+ 24			673	804	6.3
PH3DV102 PH3DV103	+ 55			632	770	6.6

EXPERIMENTAL

From the total number of 16 specimens only 14 specimens underwent successfully the large scale tests, the remaining two specimens, PH3DV101 and PH3DV104, failed during fatigue cycling (despite this fact, these two specimens were not excluded from evaluation, as can be seen e.g. from Table 3). Specimens were loaded by 4 point bending at different temperatures. For each type of material (base metal or weld metal, initial or aged condition), the temperature of the experiment was selected so that the expected fracture toughness value lie in lower part of transition region relevant for that type of material. More specifically, temperature of the experiment was selected to correspond to fracture toughness of 100 $MPam^{1/2}$. The specimens were expected to fail by cleavage fracture mechanism.
During the experiments, temperature, total force and load line displacement (LLD) were measured. Besides that, for uncladded specimens also the crack mouth opening displacement (CMOD) was recorded, while for cladded specimens only ″crack mouth strain″ (i.e. strain in direction of stress opening the crack, the strain gage being placed on the cladding surface, just above the crack mouth) was measured.
During the experiments, different specimens exhibited different behaviour. Among the uncladded specimens, specimens PHAV103, PHBV103 failed in the region of elasticity (experimental curve load vs. displacement was of linear character), specimens PHAV201, PH1CV101, PH1CV103 exhibited low or medium amount of plasticity and specimen PHBV101 exhibited large amount of plasticity. Due to lack of space we do not attach here the experimental curves force vs. LLD (CMOD) for uncladded specimens.
Cladded specimens behaved substantially different from the uncladded ones. These specimens exhibited several pop-ins during loading, these pop-ins correspond most likely to crack growth. It is assumed that the cracks propagated into cladding, but this hypothesis was not verified yet. Due to technical difficulties the cladded specimens were not numerically evaluated until now, therefore we will not present the experimental results in this paper. Both fractographic analyses and FE calculations modelling crack growth are assumed to be performed in the future.

NUMERICAL ANALYSIS OF THE EXPERIMENTS

In this chapter we attach results of numerical analyses for uncladded specimens. Evaluation of the cladded specimens is assumed to be performed in the future. Besides determination of J-integrals/K_{Jc} values, we will focus our attention to establishing also the second fracture mechanics parameter Q [1, 2], at least for two specimens containing through cracks.
Three-dimensional elastic-plastic FE analyses of uncladded specimens were performed with the SYSTUS program. Both structural (stress-strain) and post-processing fracture mechanics calculations were performed.

Description of FE meshes and plastic behaviour

For generation of meshes the ORMGEN code was used. Every mesh represents a quarter of the experimental body, with using symmetry conditions. For constructing the meshes, 3D isoparametric quadratic elements with reduced number of integration points were used. The most complex mesh contained about 3000 elements and 9000 nodes. The size of elements near the crack front (in directions perpendicular to the crack front) varied in range 0.4 - 0.9 mm. The collapsed hexahedron elements which may be optionally used to model the crack tip blunting were not used in our case. For each of the specimens, the loading was prescribed as a uniform pressure on the loading lines at the ends of the arms. Contact between test specimen and support was not modelled.
The elastic-plastic behaviour of specimens was modelled using flow theory of plasticity with von Mises yield surface and isotropic hardening. Large strains (updated Lagrangian formulation) were used.

Determination of fracture toughness for uncladded specimens

For determination of J_c-values the 3D postprocessing module of SYSTUS based on G-θ [3] method was used. We will only briefly describe some aspects of the J_c determination procedure.
To determine the moment of fracture, the calculated force vs. displacement curve is compared with the experimental one. As displacement may be taken either LLD or CMOD. In this paper we present J_c-values based mostly on force vs. CMOD curves, only in case when the accordance is not good, we use force vs. LLD curve.
For some of the semi-elliptical cracks, both J_c-values corresponding to the symmetry plane (deepest point of the crack) and maximum J_c-values (near the surface point of the crack) are attached. Since G-θ method (similarly as other methods used in commercial FE codes) produces zig-zag behaviour of J-integral along crack front, the values J_c presented here are always mean values of two nodes (corner and midside).
From value J_c the corresponding value of K_{Jc} is calculated with using the plane strain formula

$$K_J = \sqrt{(E.J/(1-\nu^2))} \qquad (1)$$

Values of J_c and K_{Jc} obtained in the way described above are summarised in Table 3.

TABLE 3
RAW FRACTURE TOUGHNESSES FOR UNCLADDED SPECIMENS
(NOT ADJUSTED TO 1T THICKNESS)

	J_c [kJm^{-2}]		K_{Jc} [MPam$^{-1/2}$]	
specimen No.	deepest point	near surface point	deepest point	near surface point
PHAV201	44.2	63.1	101	120.7
PHAV103	17.6	-	63.7	-
PHBV201	368.6	-	290.7	-
PHBV103	15.7*)	-	59.9*)	-
PH1CV101	123	150	168	186
PH1CV103	131	-	174	-
PH3DV101**)	27	-	78.9	-
PH3DV103	59.4	-	117.1	-
PH3DV104**)	19.7	-	67.3	-

*) value based on force vs. LLD curve

**) specimen failed during cycling the crack

Besides these large scale beam tests, standard type fracture toughness testing was also performed. Standard pre-cracked Charpy size (10 x 10 x 55 mm) and 1T (25 mm thick) compact specimens were tested at different temperatures. Crack size ratio a/W for all specimens lie in the region between 0.45 and 0.55.

Results of tests have been evaluated in accordance with the ASTM Test Method [3]. „Master Curve“ approach has been applied to all results. In the first step, measured fracture toughness, K_{Jc}, has been adjusted to the standard thickness of 25 mm using the relation :

$$K_{Jc(25\ mm)} = K_{min} + [K_{Jc(x)} - K_{min}] \,.\, (B_x/B_{25mm})^{1/4} \tag{2}$$

With K_{min} = 20 MPa.m$^{0.5}$ the following relation can be obtained:

$$K_{Jc(25\ mm)} = 20 + [K_{Jc(x)} - 20] \,.\, (B_x/25mm)^{1/4} \tag{3}$$

and the standard „Master Curve“ adjusted to the thickness equal to 25 mm can be expressed as:

$$K_{Jc(med)} = 30 + 70 \exp\,[0.019\,(T - T_0)], \tag{4}$$

where T is testing temperature, and T_0 is a reference temperature, both in ^oC.

All results obtained within the project have been evaluated according to the relation (4) and are summarised in Fig. 1. Together with the experimental results, mean curve representing „Master Curve“ and 1% and 99% tolerance bounds are also included. While practically all experimental data from standard type specimens lie within these tolerance bounds, most of data from large scale specimens are even higher than 99% tolerance bound. Scatter of data due to non-homogeneity of materials can be one reason for such a behaviour. Another explanation can be found in the fact that large scale specimens were tested with „shallow“ type cracks, with a/W much smaller than in standard type specimens, i.e. a/W between 0.11 and 0.29 in contrast to standard type specimens with a/W ≅ 0.5. Thus, different stress fields can be found in crack tip vicinity, which can affect final fracture toughness values. One possible explanation can be given by the potential loss of constraint due to shallow crack which may be characterised e.g. by Q-stress parameter.

Determination of Q-stress parameter

For two of the specimens containing through crack, PHAV103 and PH3DV104 (both specimens were uncladded), also the *Q*-stress parameter was calculated. In accordance with *J*-*Q* theory [1, 2], we calculated the *Q*-stress parameter, using commonly adopted definition of *Q*-stress (e.g. [4]):

$$Q = \frac{\sigma_{zz} - (\sigma_{zz})_{SSY;Q=0}}{\sigma_0} \text{ at } \theta = 0,\ \frac{r}{J/\sigma_0} = 2 \tag{5}$$

where σ_{zz} means stress opening the crack, σ_0 denotes the yield stress, *r* is distance from the crack front and $\theta = 0$ means that *Q* is calculated on the symmetry plane. Slightly different definition of *Q*-stress parameter is possible [4], in which the hydrostatic stress $\sigma_H = 1/3\ \sigma_{kk}$ is used instead of σ_{zz}.
For calculation of *Q*-stress parameter, a new, much finer mesh of the specimen had to be constructed. Two types of meshes were tested - one with element size near the crack tip of 0.08 mm, second one with the element size of 0.05 mm. The mesh near the crack front was of „radial type“ (pentahedron elements). As it was found, the values of *Q*-stress parameter were slightly dependent on the element size nearest to the crack front. In what follows, the values of *Q* corresponding to mesh size 0.05 mm are presented.
In our case, we took value $(\sigma_{zz})_{deep}$ associated with deep crack instead of $(\sigma_{zz})_{SSY,Q=0}$ in Eqn. (5), verifying previously that values $(\sigma_{zz})_{deep}$ obtained from 3D calculation for beam of the same dimensions as the tested specimens and containing deep crack (a/W = 0.5), coincide approximately (in particular, at point $r/(J/\sigma_0)$ = 2) with values of two-dimensional SSY reference solution.
Some of the results of calculations of *Q*-stress parameter for specimens PH3DV104 and PHAV103 may be seen in Figs. 2 and 3, respectively. These specimens were selected for demonstration of procedure for calculating the *Q*-stress parameter; the crack of specimen PH3DV104 is sufficiently shallow (a/W=0.12) and the constraint loss is well pronounced while the crack of the specimen PHAV103 is deeper (a/W = 0.26)

and the effect is much less pronounced.

Figs. 2 and 3 were created in such a way that σ_{zz} values relating to one node only (1st corner node nearest to the crack front) were, for different loads, plotted vs. $r/(J/\sigma_0)$, both for shallow and deep crack. Similar figures may be obtained without difficulties also for other nodes lying in close vicinity of the crack, such as 1st midside node, 2nd midside node, 2nd corner node (nearest to the crack front). But, the 1st corner node was selected in the case of specimens PH3DV104 and PHAV103, since ratio $r/(J_c/\sigma_0)$ equals approximately to 2 for r = 0.05, which is exactly the distance of 1st corner from the crack front, for each of the specimens. (Q-stress is, in general, dependent on loading (J) and we determine the Q-value in the moment of fracture, i.e. for $J=J_c$.) Thus, the *Q*-stress parameter was determined according to Eqn.(5), with $(\sigma_{zz})_{deep}$ instead of $(\sigma_{zz})_{SSY,Q=0}$, based on opening stress, resp. based on hydrostatic stress, and with using linear interpolation to get the appropriate stress values at $r/(J/\sigma_0) = 2$. In the following Table 4 this approach is denoted as approach 1.

A little different approach to determine the *Q*-stress (approach 2 in Table 4) may be applied. Within this approach, σ_{zz} values relating to different nodes for one load only (given by value of J) are plotted against $r/(J/\sigma_0)$, the load being the same for deep and shallow crack. In our case, we selected load corresponding to J~17 kJm^{-2} for specimen PHAV103 (J_c=17.5 kJm^{-2} for this specimen, see Table 3) and load corresponding to J~19 kJm^{-2} for specimen PH3DV104 (J_c=19.7 kJm^{-2} for PH3DV104), and constructed the appropriate figures. Thus, based on these figures, *Q*-stress was determined according to Eqn. (5), with $(\sigma_{zz})_{deep}$ instead of $(\sigma_{zz})_{SSY,Q=0}$, based on opening stress, resp. hydrostatic stress, and with using linear interpolation to get the appropriate stress values at $r/(J/\sigma_0) = 2$. Due to lack of space we do not attach these figures here, nevertheless the results are presented in the Table 4.

TABLE 4
CALCULATED Q-STRESSES

SPECIMEN	APPROACH	Q-STRESS	
		based on opening stress	based on hydrostatic stress
PH3DV104	1	- 0.139	- 0.141
	2	- 0.150	- 0.156
PHAV103	1	- 0.068	- 0.068
	2	- 0.080	- 0.080

Note. If the crack depth is sufficiently small (a/W ~0.1) plotting of σ_{zz} for different nodes and different loads into one figure is possible - the difference between stress values corresponding to shallow crack and those corresponding to deep crack is well pronounced. But for shallow cracks with a/W ~ 0.25 this difference is less pronounced or is not pronounced at all, and using one of the approaches described above is an efficient tool to determine the *Q*-stress.

Comparing obtained results of calculated Q-stresses for these two specimens with experimental values of fracture toughness, some tendency can be seen: specimen with negative and larger (in absolute value) Q-stress (i.e. PH3DV104) exhibits higher value of adjusted fracture toughness (86 MPa.m$^{0.5}$) in comparison with results from standard type specimens (mean value equal to 57 MPa.m$^{0.5}$) while the specimen PHAV103 that is characterised by negative and smaller (in absolute value) Q-value, got adjusted fracture toughness value (82 MPa.m$^{0.5}$) within the scatter band of standard type specimens. Thus, Q-value could be a suitable parameter for prediction or explanation of the behaviour of shallow cracks, both in test specimens and in real structures.

CONCLUSION

Evaluation of large scale tests of uncladded specimens was presented in this paper. This evaluation is not fully completed yet. Experimental results supported the assumption about the effect of shallow cracks on

fracture toughness – specimens with shallows cracks (with a/W smaller than approximately 0.20) exhibit higher fracture toughness values than specimens with standard size cracks (a/W ≅ 0.5). Rather qualitative features of determination of Q-stress parameter were described while the database of J/K_{Jc}, Q-values should be still created. Qualitatively, it was stated that Q-stress parameter is slightly mesh dependent, this problem may be solved by using the same type of mesh for all evaluations. Two approaches were suggested to evaluate the Q-stress, producing a little different values of Q-stress; approach 2 gives a little higher values of Q. However, the differences are small and their causes may lie in numerical aspects of the procedures used (e.g. linear interpolation).
Using either opening stress or hydrostatic stress in Eqn. 1 had practically no effect on Q-value, for each of the two specimens. Actually, in this case, when crack depth effect (associated with in-plane constraint) was examined, no significant effect of using either opening stress or hydrostatic stress was expected, in contrast to cases when biaxial loading or thickness effects (associated with out-of-plane constraint) are studied [5].
Since no extensive calculations of Q-stress for RPV WWER 440 steels were performed until now, Q-stress serves, for the present, only as a qualitative parameter for prediction/explanation of behaviour of specimens with shallow cracks.

References

[1] O'Dowd, N. P., Shih, C. F. (1991). *J. Mech. Phys. Solids* **39**, No. 8, 989.
[2] O'Dowd, N. P., Shih, C. F. (1992). *J. Mech. Phys. Solids* **40**, No. 5, 939.
[3] ASTM Standard Test Method for Determination of Reference Temperature, T_0, for Ferritic Steels in the Transition Range, ASTM E 1921-97
[4] Dodds, R.H. Jr., Shih, C.F., Anderson, T.L. (1993). *Int. J. Fract.* **64**, 101.
[5] Bass, B.R., McAfee, W.J., Williams, P.T., Pennell W.E. (1999). *Nuclear Engineering and Design* **188**, 259.

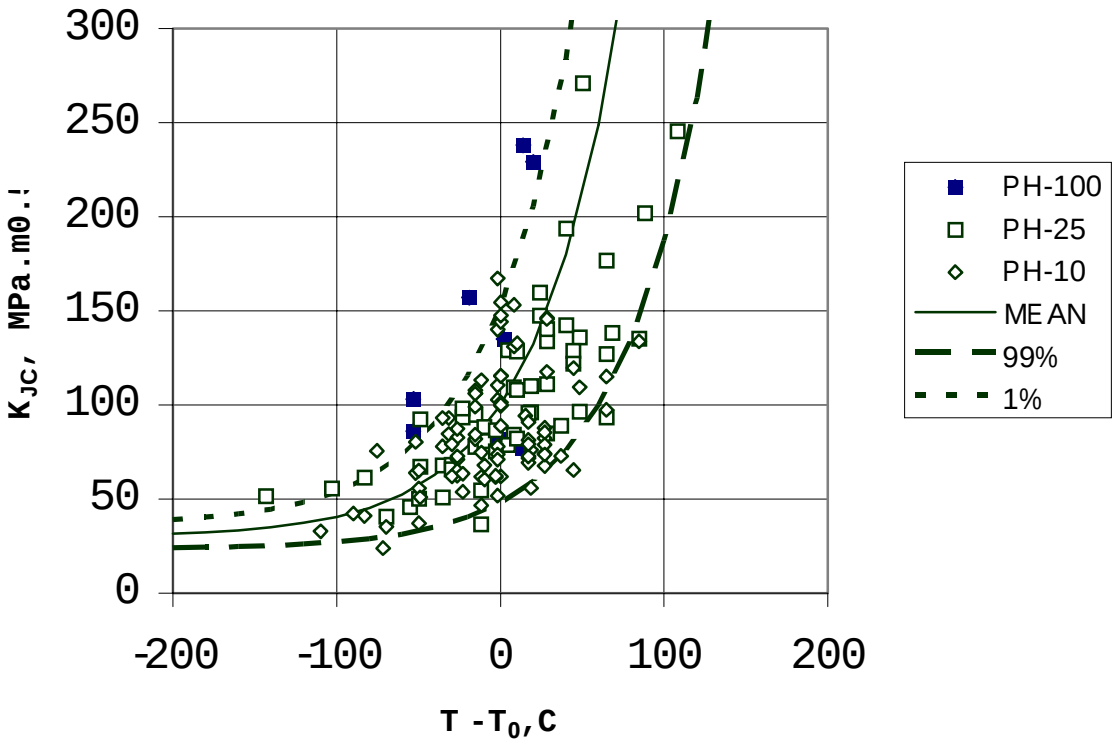

Fig. 1: Fracture toughnesses (adjusted to 1 T) of all specimens, from both large and small scale tests, as functions of T-To

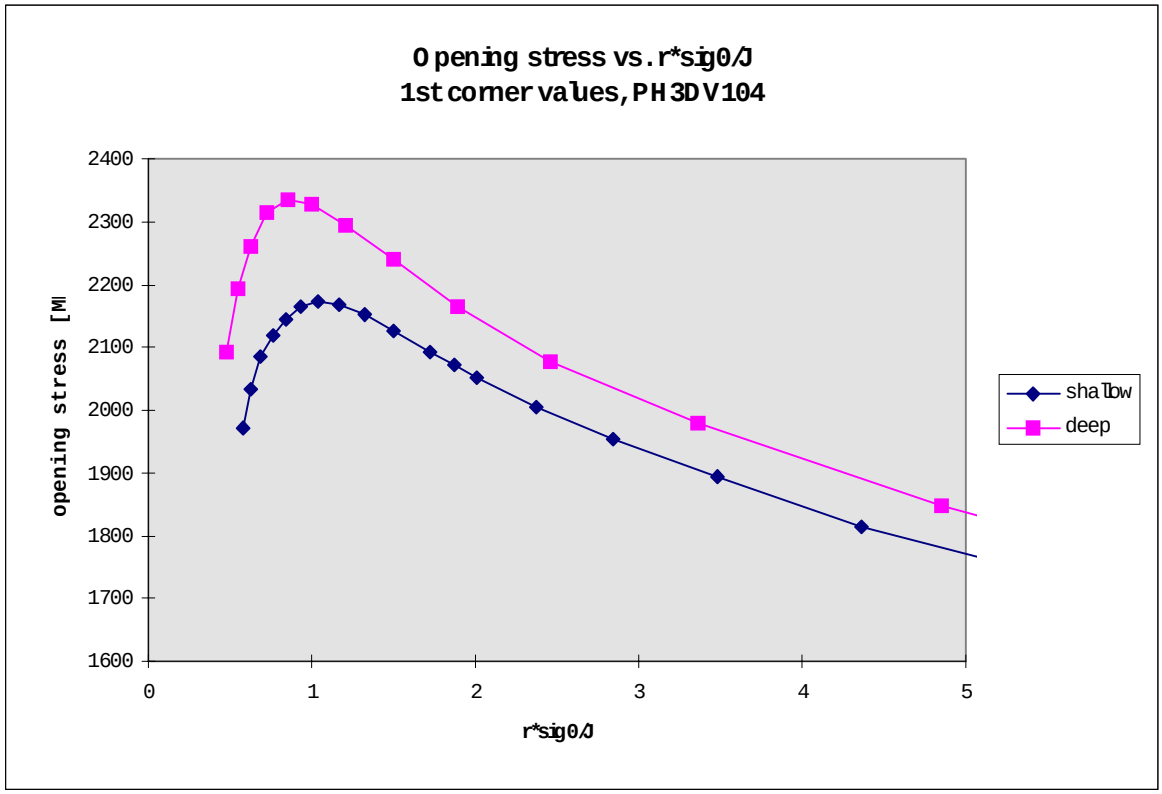

Fig. 2: Determination of Q-stress (approach 1), based on opening stress, for specimen PH3DV104

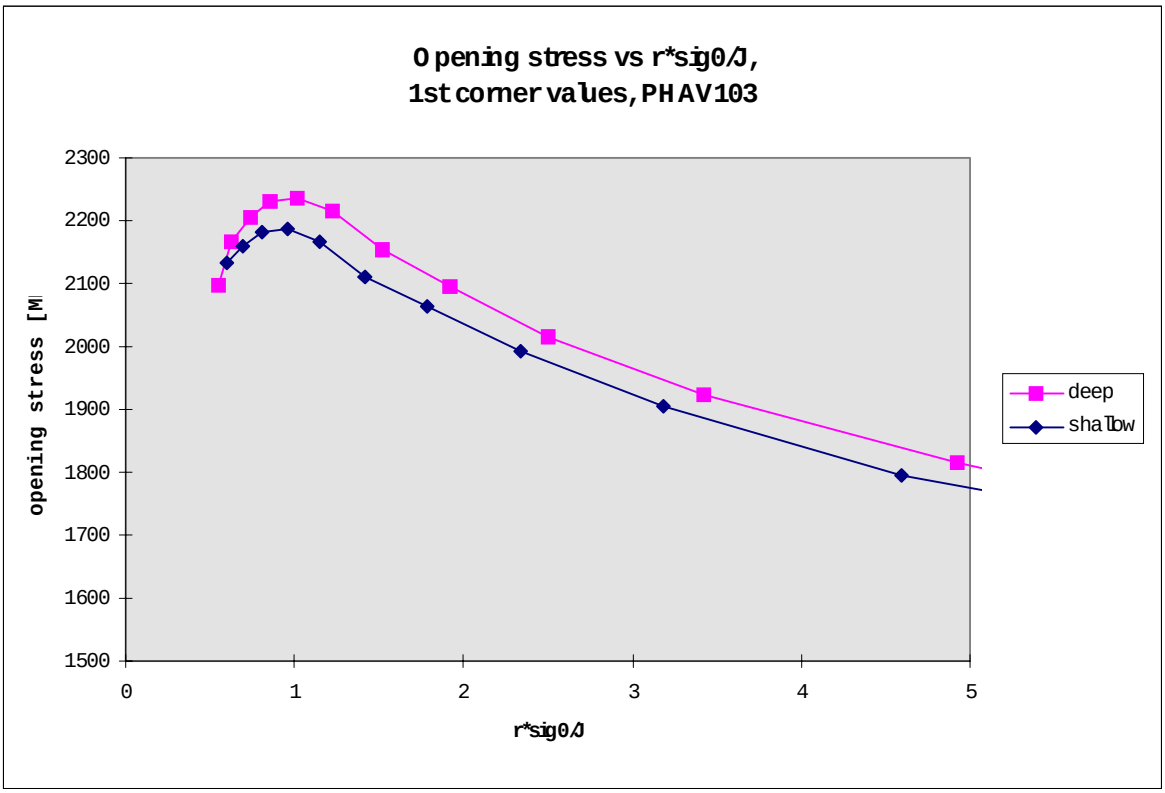

Fig. 3: Determination of Q-stress (approach 1), based on opening stress, for specimen PHAV103